Polymer Vol. 39 No. 24 pp. 6137–6143, 1998
0032-3861/98/$ – see front matter

PII: S0032-3861(98)00105-0

Surface enrichment and surface tension of oligo(styrene)/oligo(dimethylsiloxane) blends near the critical temperature

Takuhei Nose* and Naoe Kasemura
Department of Polymer Chemistry, Tokyo Institute of Technology, O-okayama, Meguro-ku, Tokyo 152, Japan
(Received 15 December 1997; accepted 27 January 1998)

Surface tensions of oligomer mixtures are theoretically and experimentally investigated in terms of surface enrichment. Surface tension is measured for blends of oligo(styrene) (OS) and oligo(dimetylsiloxane) (ODMS) as a function of composition and temperature in a one-phase region including the vicinity of critical point. With increasing ODMS content, the surface tension decreases dramatically, approaches the value of pure ODMS around 20 wt% ODMS, and then decreases very gradual, exhibiting a little sharp decrease to reach the value of pure component. The temperature dependence of the surface tension of the critical mixture is slightly weaker than those of pure polymer liquids, but shows no anomalous change near the critical point. Composition profiles and surface tension are calculated for the present system by a square-gradient theory, where the system is described as a phase-separated three-component mixture consisting polymer 1, polymer 2, and holes. The experimental results are well described by the theory. © 1998 Elsevier Science Ltd. All rights reserved.

(Keywords: surface tension; oligomer blend; surface enrichment)

INTRODUCTION

Surface enrichment in polymer blends has been an interesting issue in relation to the structure of thin films, the structure of bulk blends near the surface, and interfacial properties, such as surface tension, surface phase transitions and contact angle of wetting[1,2]. Most researches on the blend surface are focused on the microscopic structure or the composition profile at the surface. The composition profile of adsorption of the low surface-energy component at the surface has theoretically been studied by using square-gradient theories[2–6] and computational simulations[7]. Experimental studies using forward recoil spectroscopy, secondary ion mass spectroscopy and neutron reflectometry have extensively been made to see the surface enrichment, including its time dependence, in real systems[1,5,8–11]. However, direct measurements of surface tension have been limited for its importance as a fundamental surface property, probably because of experimental difficulties and lack of miscible polymer blends[6,12,13]. Dee and Sauer[6] presented the theoretical treatment of surface tension of polymer blends to compare the experimental results for blends of low and high molecular weight poly(dimethyl-siloxane) and poly(styrene)/poly(methyl vinyl ether) blends.

In this study, direct measurements of surface tension by the sessile-bubble method are performed for an oligomer blend as a function of composition and for its critical mixture near the critical temperature. When the critical point, at which the miscibility vanishes, is approached, the surface enrichment is expected to be largely enhanced owing to the reduction of capability of mixing, and the surface tension may be reduced by the surface coverage with the low surface-energy component. Theoretical description similar to, but slightly different from, the treatment of Dee and Sauer[6] is made to be compared with the experimental results. The oligomer system is the same as used in previous studies on coexistence curve[14] and interfacial tension[15], so that the location of the critical point and the interaction parameter for the blend are known.

* To whom correspondence should be addressed. Tel.: +81-3-5734-2132; fax: +81-3-5734-2888

THEORETICAL

The square-gradient theory is here adopted to describe the surface of polymer mixtures. Although the theory is applicable to an interface with a very gradual change of composition only, it is known that the theory provides a qualitatively reasonable description over a wide range of interfacial thickness. Binder *et al.*[3] and Jones *et al.*[2,4] first applied the theory to describe the composition profile of polymer blends near the surface, where the surface was in contact with a wall. Dee and Sauer[6,16] started with the equation of state for polymeric liquids to describe liquid–vapour phase equilibrium and created the liquid–vapour interface, i.e. the surface of liquid. They used the hole theory (called the lattice fluid theory) of Sanchez–Laconbe[17] or the Flory–Orwell–Vrij theory[18] as the equation of state theory to predict surface tensions of polymer liquids[16] and extended it to be applicable to polymer blend surfaces[6]. Here, we adopt the lattice fluid theory, for simplicity, and take into account both energy and entropy effects on the composition-gradient terms in the free energy, while Dee and Sauer ignored the entropy effect.

In the lattice fluid theory, the polymer liquid is described as a mixture of polymer segments and holes on a lattice, so that a binary mixture of polymer 1 and polymer 2 is described as a ternary mixture of the two polymers and

holes. Therefore, the free energy of mixing is expressed by the Flory–Huggins type theory in terms of their polymeric indices P_i, volume fractions ϕ_i and segment-interaction parameters χ_{ij} between components i and j

$$\Delta_m f = \frac{\phi_0}{P_0}\ln\phi_0 + \frac{\phi_1}{P_1\ln\phi_1} + \frac{\phi_2}{P_2}\ln\phi_2 + \chi_{01}\phi_0\phi_1 + \chi_{02}\phi_0\phi_2 + \chi_{12}\phi_1\phi_2 \quad (1)$$

Here the free energy is per lattice volume v, measured in the unit of k_BT, with k_B the Boltzmann constant, and the subscripts 0, 1 and 2 denoting the hole, polymer 1 and polymer 2, respectively. Compositions $\phi(e)$ of coexisting liquid($'$) and vapour($''$) phases at equilibrium are determined by equalities of chemical potentials $\Delta\mu_i$ of respective components

$$\Delta\mu_0{}' = \Delta\mu_0{}'' \quad (2)$$

$$\Delta\mu_1{}' = \Delta\mu_1{}'' \quad (3)$$

$$\Delta\mu_2{}' = \Delta\mu_2{}'' \quad (4)$$

The chemical potentials can be derived from the free energy of equation (1) by a conventional method, to be expressed as follows.

$$\Delta\mu_0 \frac{1}{P_0}\ln\phi_0 + \frac{(1-\phi_0)}{P_0} - \frac{\phi_1}{P_1} - \frac{\phi_2}{P_2} + \chi_{01}(1-\phi_0)\phi_1 + \chi_{02}(1-\phi_0)\phi_2 - \chi_{12}\phi_1\phi_2 \quad (5)$$

$$\Delta\mu_1 = \frac{1}{P_1}\ln\phi_1 + \frac{(1-\phi_1)}{P_1} - \frac{\phi_0}{P_0} - \frac{\phi_2}{P_2} + \chi_{01}(1-\phi_1)\phi_0 + \chi_{12}(1-\phi_1)\phi_2 - \chi_{02}\phi_0\phi_2 \quad (6)$$

$$\Delta\mu_2 \frac{1}{P_2}\ln\phi_2 + \frac{(1-\phi_2)}{P_2} - \frac{\phi_0}{P_0} - \frac{\phi_1}{P_1} + \chi_{02}(1-\phi_2)\phi_0 + \chi_{12}(1-\phi_2)\phi_1 - \chi_{01}\phi_0\phi_1 \quad (7)$$

On the basis of the square-gradient theory[19], the interfacial tension γ, that is, surface tension of the polymer blend, is given by

$$\gamma = \frac{k_BT}{v}\int(\Delta f + f_{grad})\mathrm{d}z \quad (8)$$

where the coordinate z is taken to be perpendicular to the interfacial plane, Δf is the local excess free energy due to the presence of the interface, which is a function of local composition only, and f_{grad} is the excess free energy due to the presence of composition gradients $\dot{\phi}_i = \mathrm{d}\phi_i/\mathrm{d}z$ at the interface. Δf is given from equations (5)–(7) with equation (1) as

$$\begin{aligned}\Delta f = \Delta_m f - \sum_{i=1}^{3}\left(\phi_i\Delta\mu_i(e)\right) &= \frac{\phi_0}{P_0}\ln\left(\phi_0/\phi_0(e)\right) + \frac{\phi_1}{P_1\ln}\left(\phi_1/\phi_1(e)\right) + \frac{\phi_2}{P_2\ln}\left(\phi_2/\phi_2(e)\right) \\ &- \frac{1}{P_0}\left(\phi_0\phi_0(e)\right) - \frac{1}{P_1}\left(\phi_1 - \phi_1(e)\right) \\ &- \frac{1}{P_2}\left(\phi_2 - \phi_2(e)\right) + \chi_{01}\left(\phi_0 - \phi_0(e)\right)\left(\phi_1 - \phi_1(e)\right) \\ &+ \chi_{02}\left(\phi_0 - \phi_0(e)\right)\left(\phi_2 - \phi_2(e)\right) \\ &+ \chi_{12}\left(\phi_1 - \phi_1(e)\right)\left(\phi_2 - \phi_2(e)\right) \quad (9)\end{aligned}$$

The gradient term f_{grad} is given by the sum of following entropy and energy terms, i.e. $f_{grad} = f^s_{grad} + f^e_{grad}$[19–21]

$$f^s_{grad} = \frac{a_1^2}{36\phi_1}\dot{\phi}_1^2 + \frac{\alpha_2^2}{36\phi_2}\dot{\phi}_2^2 \quad (10)$$

$$f^e_{grad} = \frac{\chi_{01}\lambda_{01}^2}{2}\dot{\phi}_0\dot{\phi}_1 + \frac{\chi_{02}\lambda_{02}^2}{2}\dot{\phi}_0\dot{\phi}_2 + \frac{\chi_{12}\lambda_{12}^2}{2}\dot{\phi}_1\dot{\phi}_2 \quad (11)$$

where a_i is the statistical segment length, and λ_{ij} represents the range of distance within which the interaction between i and j segments is working. Transforming the polymer fractions ϕ_i into the polymer composition $\theta = \theta_1 = \phi_1/(\phi_1 + \phi_2)$ with

$$\phi_1 = (1-\phi_0)\theta;\ \ \phi_2 = (1-\phi_0)(1-\theta) \quad (12)$$

the interfacial tension is finally given by

$$\gamma = \frac{k_BT}{v}\int I\ \mathrm{d}z \quad (13)$$

with

$$I \equiv \Delta f + g\dot{\phi}_0^2 + h\dot{\theta}^2 + k\dot{\phi}_0\dot{\theta} \quad (14)$$

where

$$g = \frac{1}{2}\left\{\chi_{01}\lambda_{01}^2\theta + \chi_{02}\lambda_{02}^2(1-\theta) - \chi_{12}\lambda_{12}^2\theta(1-\theta)\right\} + \frac{\alpha_1^2\theta + \alpha_2^2(1-\theta)}{36(1-\phi_0)} \quad (15)$$

$$h = \frac{1}{2}\chi_{12}\lambda_{12}^2(1-\phi_0)^2 + \frac{1}{36}(1-\phi_0)\left(\frac{\alpha_1^2}{\theta} + \frac{\alpha_2^2}{1-\theta}\right) \quad (16)$$

$$k = \frac{1}{2}\left\{\chi_{02}\lambda_{02}^2 - \chi_{01}\lambda_{01}^2 + \chi_{12}\lambda_{12}^2(1-2\theta)\right\} - \frac{1}{18}\left(\alpha_1^2 - \alpha_2^2\right) \quad (17)$$

Minimizing the surface excess free energy γ given by equation (13), one can obtain the composition profiles at the interface and the value of γ at equilibrium. Euler's equations for minimizing the integral are

$$\frac{\partial I}{\partial\phi_0} - \frac{\mathrm{d}}{\mathrm{d}z}\left\{\frac{\partial I}{\partial\dot{\phi}_0}\right\} = 0 \quad (18)$$

$$\frac{\partial I}{\partial\theta_1} - \frac{\mathrm{d}}{\mathrm{d}z}\left(\frac{\partial I}{\partial\dot{\theta}_1}\right) = 0 \quad (19)$$

Also the following equation holds

$$I - \left[\dot{\phi}_0\left(\frac{\partial I}{\partial\dot{\phi}_0}\right) + \dot{\theta}\left(\frac{\partial I}{\partial\dot{\theta}}\right)\right] = 0 \quad (20)$$

which leads to

$$\Delta f = g\dot{\phi}_0^2 + h\dot{\theta}^2 + k\dot{\phi}_0\dot{\theta}\ \ I = 2\Delta f \quad (21)$$

Therefore, one has

$$\gamma = \frac{2kT}{\nu}\int\Delta f\ \mathrm{d}z \quad (22)$$

Solving the simultaneous equations of either equations (18) and (19) or equation (21) and one of equations (18) and (19), one can determine θ and ϕ_0 as functions of z and evaluate γ by equation (22).

EXPERIMENTAL

Materials and samples

The blends were a mixture of oligo(dimethylsiloxane) (ODMS) and oligostyrene (OS), which were the same as used in our previous papers[14,15]. ODMS was a product of Shin-etsu Co. Ltd, with the number-average molecular weight M_n of 460. It was substantially the pentamer with narrow molecular-weight distribution. OS was a product of Pressure Chemical Co. with the weight-average molecular weight M_w = 600 and the polydispersity index $M_w/M_n < 1.10$. The mixture of ODMS/OS has an upper critical solution temperature at 101.92°C and the critical composition of ODMS is 0.50 in weight fraction (0.55_7 in volume fraction)[14].

Surface tension measurements

Surface tension was measured by using the sessile-bubble method. The apparatus and experimental procedures were similar to those used in the previous study on interfacial tension by the sessile-drop method[15]. The apparatus is schematically illustrated in *Figure 1*. A nitrogen-gas bubble was formed on a plate in blend liquid in a glass cell. The image of the bubble was focused on the detector of a CCD camera, and its size and profile were measured by image analysis. The blended sample with a desired composition was sealed in the glass cell, and homogenized at about 150°C in one phase region above the critical temperature. Temperature was controlled to within ± 0.05°C.

The value of $\gamma/g\Delta\rho$, g and $\Delta\rho$ being the gravity constant, and density difference between the sample liquid and the nitrogen gas, respectively, was evaluated from size and profile of the bubble by fitting to those computed by the Laplace equation[20]. Surface tension γ was calculated from the values of $\gamma/g\Delta\rho$ with $\Delta\rho$. The $\Delta\rho$ was assumed to be equal to the density of the sample liquid and evaluated from those of pure OS and ODMS[14], assuming the additivity of density for mixtures. It took a little time for the bubble to have equilibrium shapes. The surface tension calculated for a bubble was stabilized around 30 min after making the bubble as shown in *Figure 2*, so that the bubble was stayed for 1 h at measuring temperatures, and then the bubble profile was recorded.

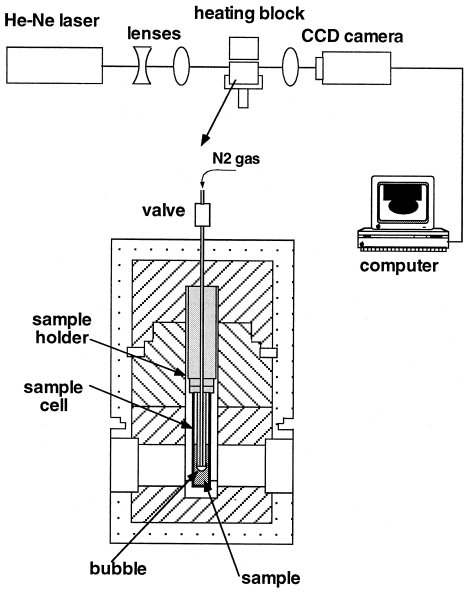

Figure 1 Schematic illustration of the apparatus of surface tension measurements

RESULTS AND DISCUSSION

Experimental results

Composition dependence. Surface tensions at 130°C and 110°C are plotted as a function of ODMS weight fraction in *Figure 3*. With increasing content of ODMS with lower surface tension, the surface tension of the mixture decreases sharply to almost the same value as that of pure ODMS around 20 wt% ODMS, then gradually decreases, and reaches the value of pure ODMS with a little stronger decrease near 100 wt% ODMS.

Because of large difference in γ and poor miscibility between OS and ODMS, the decrease of γ with addition of ODMS is very steep, and the value of γ for the critical mixture of about 59 wt% of ODMS is fairly close to that of ODMS. The shape of the γ-composition curve near the 100% of low energy component is similar to that observed for poly(styrene)/poly(vinylmethylether)[6].

Temperature dependence. Temperature dependences of γ for pure OS, pure ODMS, and the mixture with the critical composition are shown in *Figure 4*. For the pure oligomers, the temperature dependence is expressed by the following linear relations in the present experimental temperature range (90–140°C).

OS $\quad \gamma/(\text{mN m}^{-1}) = 38.8 - 0.069T/\text{K}$

ODMS $\quad \gamma/(\text{mN m}^{-1}) = 16.8 - 0.051T/\text{K}$

On the contrary, the critical mixture has a little weaker temperature dependence, and seems to show a slightly stronger increase in γ near the critical temperature T_c as the

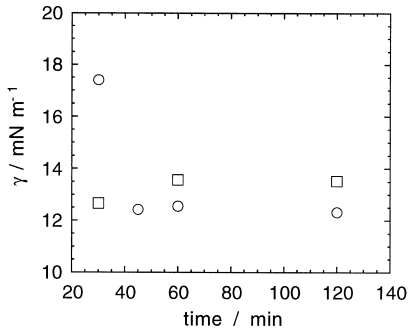

Figure 2 Time dependence of surface tension γ: ○, at 130°C; □, at 110°C

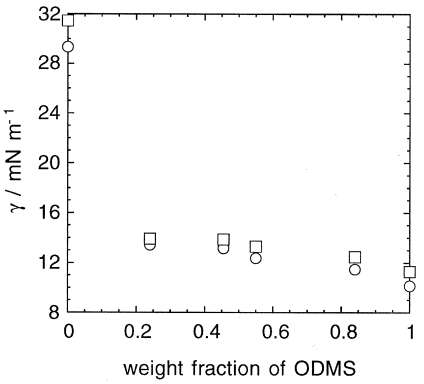

Figure 3 Surface tension γ against weight fraction of ODMS: ○, at 130°C; □, at 110°C

temperature decreases to approach T_c. The temperature dependence of surface tension for liquids is often expressed by the MacLeod exponent n defined by[22,23]

$$\gamma = [P](\Delta\rho)^n \tag{23}$$

where $[P]$ is a material-dependent constant called the parachor and $\Delta\rho$ is again the density difference between liquid and vapour phases. The MacLeod exponent obtained from the experimental data is 4.5 for OS, 4.2 for ODMS, and 2.6 for the critical mixture at temperatures $T > 110$°C. The values for OS and ODMS fall in the range of typical values for polymer melts ranging from 3.0 to 4.4[24,25], while that of the critical mixture is smaller, indicating the presence of surface-enrichment effects, which will be discussed later.

Theoretical calculations

Values of parameters required for the calculations are the polymeric indices P, the statistical segment length a, the interaction length λ, and the interaction parameters χ. Taking the volume of OS monomer($\nu = 103.3$ml mol^{-1}) as the lattice volume v, one has $P_0 = 1$, $P_1 = 5.57$ and $P_2 = 5.77$, and the literature gives $a_1 = a_2 = 0.683$ nm(accidentally $a_1 = a_2$), where the subscripts 1 and 2 denote ODMS and OS, respectively[15]. The parameter χ_{12} for the present blend of OS/ODMS is given by $\chi_{12}/v/(\text{mol ml}^{-1}) = 1.849/(T/\text{K}) - 0.00143$ as a function of the absolute temperature T[14], so that $\chi_{12} = 0.33$ at 400 K(≅ 127°C), for example. The λ-value cannot easily be estimated, so that we put $\lambda_{01}^2 = \lambda_{02}^2 = \lambda_{12}^2 = 0.25\,\text{nm}^2$ tentatively, since the interaction length must be of the same order of segment size. The other unknown parameters are χ_{01} and χ_{02}, which are determined so as to reproduce the experimental γ values of pure components OS and ODMS, respectively. The obtained values are $\chi_{01} = 2.4$ and $\chi_{02} = 4.2$ at 400 K.

Calculations are carried out in the following procedures. Compositions of equilibrium coexistence phases are first computed from equations (2)–(4) with equations (5)–(7). Then, the simultaneous differential equations are solved with a given set of initial values of ϕ_0, θ, and their gradients at a position in the vapour phase away from the centre of interface. By trail and error with changing the initial values, one can obtain the stable solutions that give values of ϕ_0 and θ as functions of z correspond to the composition profiles, providing the excess free energy Δf as a function of z to yield the surface tension by equation (22). The intrinsic length scale of the surface profile is essentially determined by the parameters a and λ. The theory assumes a blend of flexible long-chain polymers, which yields the entropic gradient term f^s_{grad} of equation (10). Since the present system is an oligomer mixture, the term f^s_{grad} is not quantitatively relevant here. This irrelevancy and the arbitrariness in putting the λ-value bring about some fuzziness in the quantitative results of the present calculations.

Composition dependence. Calculated results for surface tension at a temperature ($\chi = 0.33$, $T = 400$ K) above the critical point are shown as a function of blend composition of ODMS, C_{ODMS}, in volume fraction in *Figure 5*, along with the experimental results for comparison. Also shown are calculated curves by a monolayer model proposed by Prigogine and Marechal[26,27], where only the first lattice layer is regarded as the surface with polymer composition different from that of the bulk phase. Details of the calculation are described in Appendix. The present square-gradient theory describes the experimental composition dependence of γ well, even reproducing the downturn near the 100% ODMS composition. The monolayer also gives a fairly good description for the composition dependence of γ. However, the present theory gives much better results.

In *Figure 6*, examples of calculated composition profiles at the surface are illustrated as a function of blend composition C_{ODMS}, which is equivalent to the bulk composition θ_{bulk} ($\theta_{\text{bulk}} \equiv C_{\text{ODMS}}$). The position $z = 0$ is set at $\phi_0 = 1 - \phi_0 = 0.5$. The surface layer, where the polymer density, $1 - \phi_0$, is sharply changing, has a thickness of about 1 nm. Even at a low blend composition of ODMS, the top surface of the surface layer is almost 100% covered with the lower surface-energy component, ODMS, although the ODMS density is not as high as that of the pure bulk ODMS. The surface enriched layer, where the ODMS composition is higher than that of the bulk phase, has a thickness of a couple of nm.

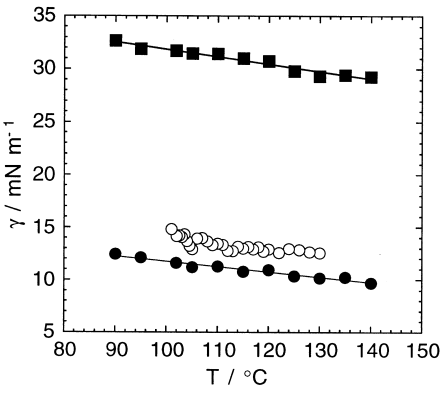

Figure 4 Temperature dependence of surface tension γ: ■, OS; ●, ODMS; ○, the critical mixture of OS/ODMS (50/50 in wt%). Straight lines are obtained by the least-squares fitting, of which equations are described in the text

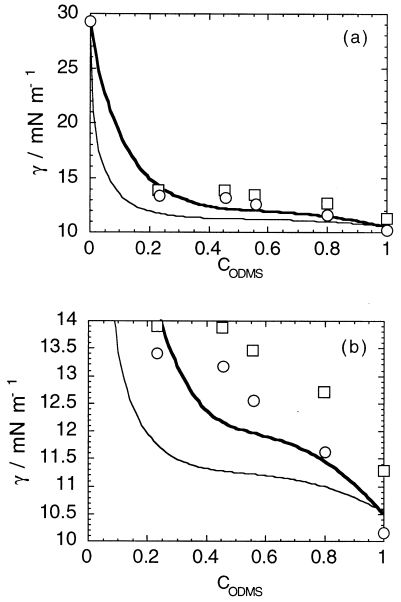

Figure 5 Blend-composition (C_{ODMS}) dependence of surface tensions for OS/ODMS blends. Plots are experimental data at 130°C (○) and 110°C (□). Thick and thin lines are calculated by the square-gradient theory and the monolayer model at 400 K(~127°C), respectively. (b) is an enlarged presentation of (a). The parameters used in calculations are described in the text

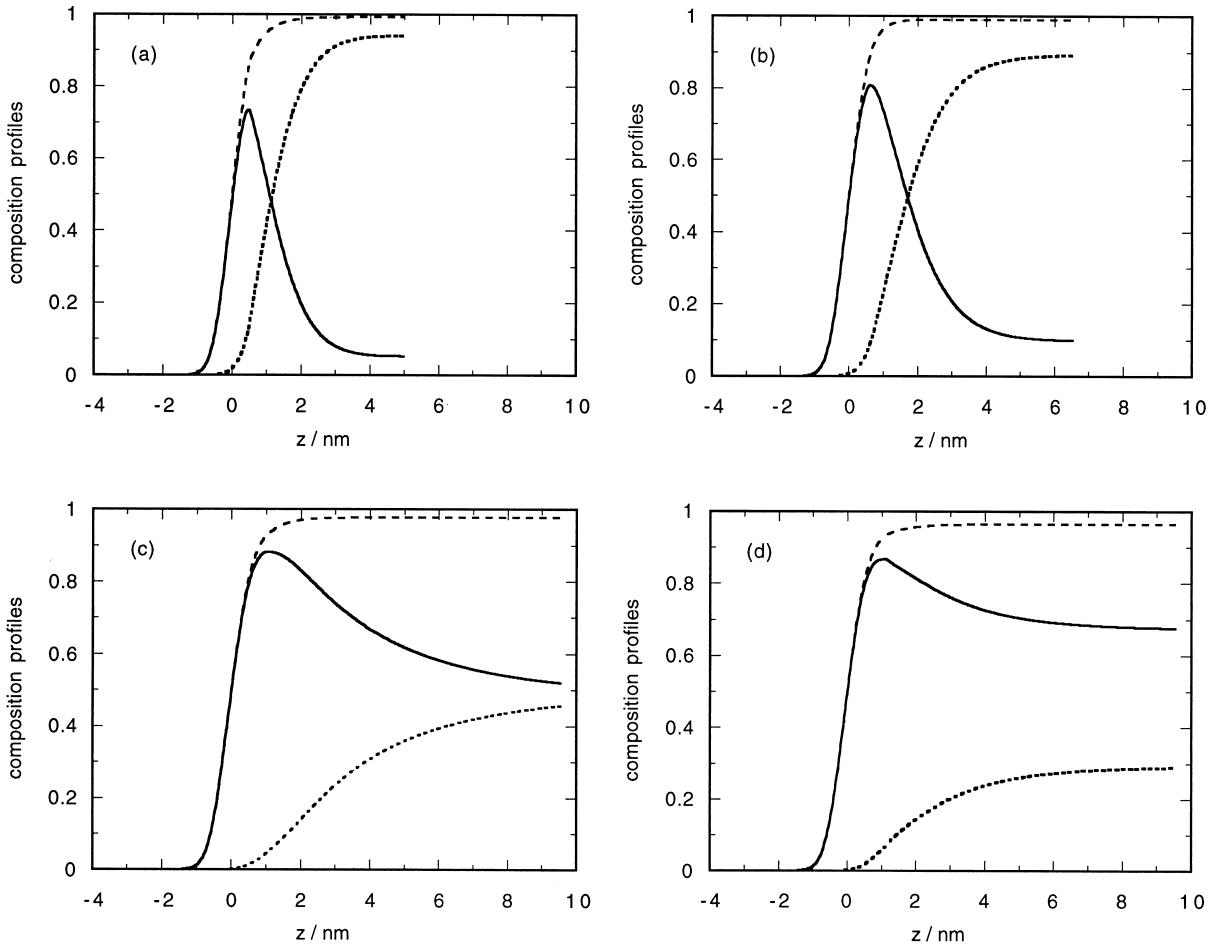

Figure 6 Surface composition profiles for ODMS/OS blends calculated by the square-gradient theory as a function of blend composition. Solid, dotted and broken lines denote the volume fractions of ODMS, OS and the total oligomer, respectively, at $\chi_{12} = 0.33$ (400 K). Blend compositions C_{ODMS} ($= \theta_{\mathrm{bulk}}$) are 0.05, 0.1, 0.5 and 0.7 for (a), (b), (c) and (d), respectively.

Profiles of adsorbed ODMS can be represented by the excess fraction θ^* of ODMS at the surface defined as $\theta^* = (\theta - \theta_{\mathrm{bulk}})/(1 - \theta_{\mathrm{bulk}})$ being a function of z, which are illustrated in *Figure 7*. As the blend composition C_{ODMS} ($= \theta_{\mathrm{bulk}}$) increases, the ODMS enriched layer becomes thicker (*Figure 7*), and the peak of the profile of ODMS (*Figure 6*) becomes broader. As the composition approaches the pure ODMS, the surface enriched layer becomes thinner again. This can reasonably be understood if one notices the following general expectation. The thickness of the surface enriched layer can be reworded to be the length of tail of the composition recovering from the surface composition to the bulk composition (*Figure 7*). The driving force of the recovery is nothing other than the miscibility, approximately being expressed by the second derivative of the mixing free energy with respect of the composition, $\partial^2\Delta_{\mathrm{m}}f/\partial\theta^2$. Therefore, the higher (or lower) miscibility gives the shorter (or longer) recovery, resulting in the shorter (or longer) tail, that is, the thinner (or thicker) surface enriched layer. Since the smaller amount of solute (minor component) is generally more 'miscible' with solvent (major component) than the larger amount. This causes less surface enrichment at compositions closer to the pure component. This may also be responsible for the downturn of γ-ODMS composition curve near pure ODMS.

Temperature dependence. *Figure 8* represents theoretically calculated results for the temperature dependence of the critical mixture, where the normalized interfacial tension γ_{n} defined as $(\gamma - \gamma_{\mathrm{ODMS}})/(\gamma_{\mathrm{OS}} - \gamma_{\mathrm{ODMS}})$ is used, with γ_{ODMS} and γ_{OS} being, respectively, the surface tensions of pure ODMS and OS, along with the experimental results for comparison. The theories predict that γ_{n} decreases as the critical temperature is approached. This agrees with the small MacLeod's exponent and with the experimental results shown in *Figure 8*, although the data are scattered and exhibit a weak upturn near the critical point. The theoretical curves seem to have no singularity at the critical point, but show rather weakly enhanced decrease in surface

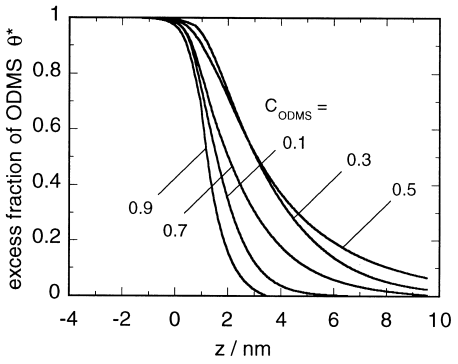

Figure 7 Adsorption profiles of ODMS in ODMS/OS blend surfaces expressed by the excess fraction of ODMS[$(\theta - \theta_{\mathrm{bulk}})/(1 - \theta_{\mathrm{bulk}})$] as a function of the position z at 400 K. Numbers denote the blend composition of ODMS (C_{ODMS}) equivalent to the composition (θ_{bulk}) in polymer bulk phase

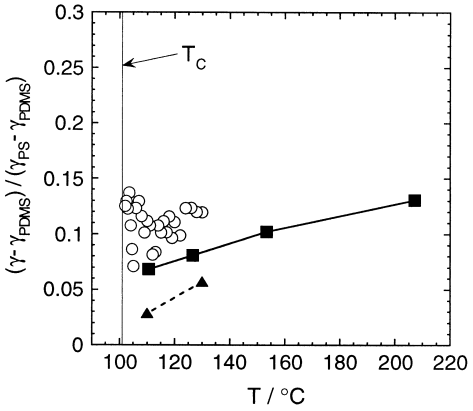

Figure 8 Temperature dependence of normalized surface tension for the critical mixture of OS/ODMS (50/50 in wt%): ■, calculated by the square-gradient theory; ▲, calculated by the mono-layer model; ○, experimental data. Critical temperature is 101.92°C

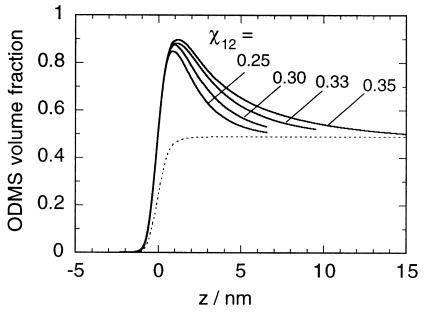

Figure 9 Temperature dependence of surface composition profiles of the critical ODMS/OS mixture calculated by the square-gradient theory. Solid lines are the volume fractions of ODMS at χ_{12} values of indicated numbers. (Note that $\chi = 0.3528$ at the critical point under the mean-field approximation. Dotted line indicates $(\phi_1 + \phi_2) \times$ (bulk ODMS composition), which is supposed to be the ODMS profile with no adsorption

tension. The upturn of the experimental data near the critical point might be due to the critical fluctuations, but we can say nothing definite because of poor quality of the data.

In *Figure 9* are shown composition profiles of ODMS as a function of temperature, i.e. of the χ-value. When the critical point is approached, the surface enrichment is pronounced and the tail of composition decay to the bulk one becomes longer. The tail length or the thickness of surface enriched layer becomes infinitely large at the critical point, since the miscibility vanishes there (see the argument made above for the composition dependence). However, the surface tension is primarily determined by the surface enrichment at the very surface, so that the decrease in surface tension near the critical is not so drastic as the increase in the thickness of the surface enriched layer.

CONCLUSIONS

Surface tensions of oligomer blends have successfully been measured as functions of composition and temperature, including the vicinity of the critical point. In the critical mixture, the temperature dependence of surface tension is weak compared with those of pure oligomers, but no dramatic decrease in surface tension is observed near the critical point. With increasing content of the low surface-energy component ODMS at a constant temperature above the critical point, the surface tension decreases very quickly to be close to the surface tension of pure ODMS, then very gradually decreases, and reaches the value of pure component with a little sharp decrease. Using a square-gradient theory, surface tensions and composition profiles are calculated for the present system. The theory describes the observed behaviour of surface tension well. According to the theoretical calculations, the thickness of the surface enriched layer becomes larger and larger when the critical point is approached, as expected. However, the surface tension decreases very gradually, being less sensitive to the miscibility of the blend.

APPENDIX A: MONOLAYER LATTICE MODEL FOR SURFACE ADSORPTION

On the basis of a monolayer model for the surface of polymer solution proposed by Prigogine and Marehcal[25], Gaines[26] derived the formulas for the surface tension and polymer concentration at the surface layer. In this theory, the surface layer, where the segment concentration is different from that of the bulk phase, is assumed to be the first layer at the surface only, and no conformational and combinatorial entropy changes due to the presence of inhomogeneity near the surface are taken into account. Extending the theory to a polymer/polymer mixture, one can obtain the chemical potentials per segment in bulk and at the surface as follows.

$$\mu_1 = \mu_1^0 + \frac{RT}{P_1}\left[\ln \phi_1 + \left(1 - \frac{P_1}{P_2}\right)\phi_2\right] + RT\chi\phi_2^2 \qquad \text{(A-1)}$$

$$\mu_2 = \mu_2^0 + \frac{RT}{P_2}\left[\ln \phi_2 + \left(1 - \frac{P_2}{P_1}\right)\phi_1\right] + RT\chi\phi_1^2 \qquad \text{(A-2)}$$

$$\mu_1^s = \mu_1^{0s} + \frac{RT}{P_1}\left[\ln \phi_1^s + \left(1 - \frac{P_1}{P_2}\right)\phi_2^s\right] - \gamma N\alpha$$

$$\mu_2^s = \mu_2^{0s} + \frac{RT}{P_2}\left[\ln \phi_2^s + \left(1 - \frac{P_2}{P_1}\right)\phi_1^s\right] - \gamma N\alpha \qquad \text{(A-3)}$$

where the superscript *s* indicates the surface layer, *a* is the statistical segment length, here assumed common for polymers 1 and 2, *N* is the Avogadro constant, and the other symbols are the same as those in the main text. Putting $\mu_1 = \mu^s{}_1$ and $\mu_2 = \mu^s{}_2$ of equilibrium conditions, one obtains the equations of γ and the surface segment concentration $\phi^s{}_1$ as

$$\gamma = \gamma_1^0 + \frac{kT}{\alpha}\left[\frac{1}{P_1}\ln\frac{\phi_1^s}{\phi_1} + \left(\frac{1}{P_1} - \frac{1}{P_2}\right)(\phi_2^s - \phi_2) - \chi(\phi_2)^2\right]$$
$$= \gamma_2^0 + \frac{kT}{\alpha}\left[\frac{1}{P_2}\ln\frac{\phi_2^s}{\phi_2} + \left(\frac{1}{P_2} - \frac{1}{P_1}\right)(\phi_1^s - \phi_1) - \chi(\phi_1)^2\right] \qquad \text{(A-4)}$$

$$\frac{P_2\phi_1^s}{P_1(1-\phi_1^s)} = \frac{P_2\phi_1}{P_1(1-\phi_1)}\exp\left[\frac{\alpha}{kT}(\gamma_2^0 - \gamma_1^0) + \chi(1-2\phi_1)\right] \qquad \text{(A-5)}$$

where γ_1^0 and γ_2^0 are the surface tensions of pure components. Giving the same values for P_1, P_2, $a(= a_1 = a_2)$, and $\chi(= \chi_{12})$ as those used for the square-gradient theory in the main text, the surface tension was calculated by equation (A-4) with equation (A-5) and the measured values of γ_1^0 and γ_2^0.

REFERENCES

1. Cahn, J. W., *Chem. Phys.*, 1977, **66**, 3667.
2. Jones, R. A. L., Kramer, E. J., Rafailovich, M. H., Sokolov, J. and Schwartz, S. A., *Phys. Rev. Lett.*, 1989, **62**, 280.
3. Schmidt, I. and Binder, K., *J. Physique*, 1985, **46**, 1631.
4. Jones, R. A. L. and Kramer, E. J., *Polymer*, 1993, **34**, 115.
5. Kumer, S. K. and Russell, T. P., *Macromolecules*, 1991, **24**, 3816.
6. Dee, G. T. and Sauer, B. B., *Macromolecules*, 1993, **26**, 2771.
7. Wang, J. S. and Binder, K., *J. Chem. Phys.*, 1991, **94**, 8537.
8. Thomas, H. R. and O'Malley, J. J., *Macromolecules*, 1979, **12**, 323.
9. Pan, D. H. K. and Prest, M. Jr, *J. Appl. Phys.*, 1985, **58**, 2861.
10. Hopkinson, I., Kiff, F. T., Richards, R. N., Affrossman, S., Hartshorne, M., Pethrick, R. A., Munro, H. and Webster, J. R. P., *Macromolecules*, 1995, **28**, 627.
11. Geoghegan, M., Nicolai, T., Penfold, J. and Jones, R. A. L., *Macromolecules*, 1997, **30**, 4220.
12. Rastogi, A. K. and St Pierre, L. E., *J. Colloid Interface Sci.*, 1969, **31**, 168.
13. LeGrand, D. G. and Gaines, G. L. Jr, *J. Polym. Sci.*, 1971, **C34**, 45.
14. Nose, T., *Polymer*, 1995, **36**, 2243.
15. Nose, T., *Macromolecules*, 1995, **28**, 3702.
16. Sauer, B. B. and Dee, G. T., *Macromolecules*, 1991, **24**, 2124; Dee, G. T. and Sauer, B. B., *J. Colloid Interface Sci*., 1992, **152**, 85.
17. Sanchez, I. C. and Lacombe, R. H., *J. Phys. Chem.*, 1976, **80**, 2352.
18. Flory, P. J., Orwoll, R. A. and Vrij, A., *J. Amer. Chem. Soc.*, 1964, **86**, 3515.
19. Cahn, J. W. and Hilliard, J. E., *J. Chem. Phys.*, 1958, **28**, 258.
20. Nose, T., *Polym. J.*, 1976, **8**, 96.
21. Joanny, J. F. and Leibler, L., *J. Phys. (Paris)*, 1978, **39**, 951.
22. Adamson, A. W., *Physical Properties of Surfaces*, 5th edn. John Wiley, New York, 1990, Ch. II.
23. MacLeod, D. B., *Trans. Faraday Soc.*, 1923, **19**, 38.
24. Nose, T., *Polymer J.*, 1972, **3**, 1.
25. Wu, S., *Polymer Blends*, ed. D. R. Paul and S. Newman, Vol. 1. Academic Press, New York, 1978, Ch. 6.
26. Prigogine, I. and Marechal, J., *J. Colloid Sci.*, 1952, **7**, 122.
27. Gaines, G. L. Jr, *J. Phys. Chem.*, 1969, **73**, 3143.